Journal of Comparative Physiology B
https://doi.org/10.1007/s00360-023-01513-5

ORIGINAL PAPER

Circadian gene transcription plays a role in cellular metabolism in hibernating brown bears, *Ursus arctos*

Ellery P. Vincent[1] · Blair W. Perry[1] · Joanna L. Kelley[2] · Charles T. Robbins[1,3] · Heiko T. Jansen[1,4]

Received: 29 June 2023 / Revised: 28 August 2023 / Accepted: 5 September 2023

Abstract

Hibernation is a highly seasonal physiological adaptation that allows brown bears (*Ursus arctos*) to survive extended periods of low food availability. Similarly, daily or circadian rhythms conserve energy by coordinating body processes to optimally match the environmental light/dark cycle. Brown bears express circadian rhythms in vivo and their cells do in vitro throughout the year, suggesting that these rhythms may play important roles during periods of negative energy balance. Here, we use time-series analysis of RNA sequencing data and timed measurements of ATP production in adipose-derived fibroblasts from active and hibernation seasons under two temperature conditions to confirm that rhythmicity was present. Culture temperature matching that of hibernation body temperature (34 °C) resulted in a delay of daily peak ATP production in comparison with active season body temperatures (37 °C). The timing of peaks of mitochondrial gene transcription was altered as were the amplitudes of transcripts coding for enzymes of the electron transport chain. Additionally, we observed changes in mean expression and timing of key metabolic genes such as *SIRT1* and *AMPK* which are linked to the circadian system and energy balance. The amplitudes of several circadian gene transcripts were also reduced. These results reveal a link between energy conservation and a functioning circadian system in hibernation.

Keywords Hibernation · Circadian rhythm · Metabolism · Brown bear · Transcription

Introduction

As the earth rotates on its axis, it creates a predictable 24-h cycle that is evident with the sunrise and sunset. These environmental rhythms have been internalized to create 'clocks' capable of coordinating organismal physiology with predictable environmental patterns such as the day/night cycle (Aschoff 1960). Specifically, *circa*dian (about a day) rhythms aid in coordinating animal behavior and physiology with daily environmental cues (Buhr et al. 2010) and circadian rhythms are closely linked to the control of metabolic systems (Rutter et al. 2002). These clocks are found in most, if not all, cells of the body and are generated via transcriptional–translational feedback loops (TTFLs; Supplemental Fig. 1) (Dunlap 1999; Lowery and Takahashi 2004). The circadian control of metabolism via interactions with clock TTFLs is energetically advantageous by timing cellular processes to expected environmental fluctuations, which allows organisms the ability to alter their ATP production to when energy is most needed (Bass and Takahashi 2010), for example during the sleep–wake cycle. Consequently, the benefits of expressing circadian rhythms must outweigh the energetic costs associated with producing them.

Hibernation in bears is an adaptation that benefits animal survival through periods of low food availability by using adipose as an energy source (Robbins et al. 2012). In brown bears, reductions in body temperature (Tb, active 37 °C, hibernation 30–34 °C), activity (greater than 90%), and oxygen consumption rate (up to 75%) enables bears to significantly reduce their energy expenditure (Welinder et al. 2016; Tøien et al. 2011; Robbins et al. 2012) while avoiding

Communicated by G. Heldmaier.

✉ Heiko T. Jansen
heiko@wsu.edu

[1] School of Biological Sciences, Washington State University, Pullman, WA 99163, USA

[2] Ecology and Evolutionary Biology, University of California Santa Cruz, Santa Cruz, CA 95060, USA

[3] School of the Environment, Washington State University, Pullman, WA 99163, USA

[4] Department of Integrative Physiology and Neuroscience, Washington State University, Pullman, WA 99163, USA

Published online: 11 October 2023

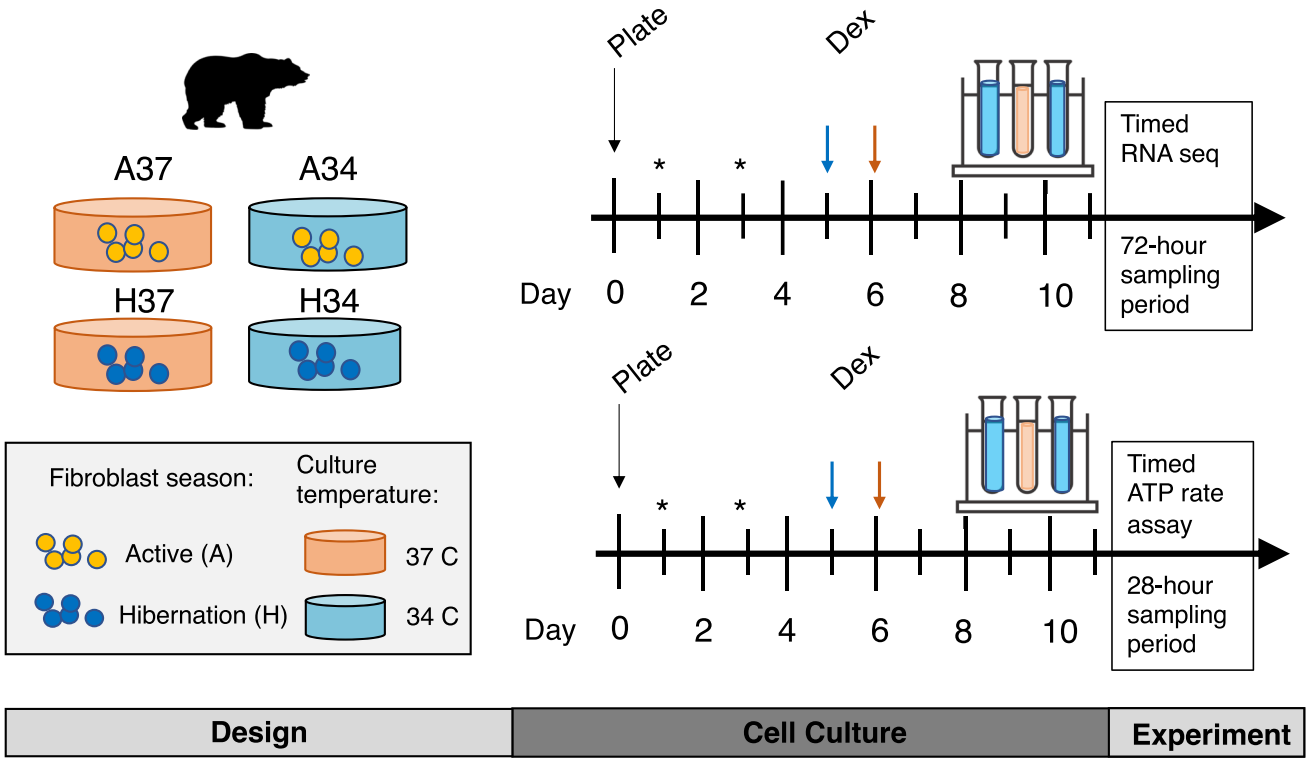

Fig. 1 Visual schematic showing experimental design for both timed rhythmic RNAseq and ATP rate experiments. Both experiments utilized four experimental conditions which incorporated two different season types (active and hibernation), and two different culture temperatures (34 °C and 37 °C). Medium was changed (represented by a (*)) 50% 24 h after plating, and every 48 h until confluency. 48 h prior to experimental sampling, all cells were synchronized with dexamethasone, indicated by the arrows. ATP experiments were quantified every 4 h for a period of 28 h ($N=6$), and RNAseq was sampled every 3 h for a period 72 h ($N=1$). See METHODS for additional details

pathology (Nelson et al. 1973). Unlike bears, rodent hibernators experience reduction in metabolism that is characterized by bouts of torpor (Tb ~ 0° −30 °C) and periods of arousal that bring core Tb back to euthermic levels (37 °C; Körtner and Geiser 2000; Williams et al. 2012). These small hibernators lose circadian rhythmicity during torpor (Williams et al. 2017; Revel et al. 2007), while brown bears retain circadian rhythms of Tb, activity, and gene expression (Jansen et al. 2016; Ware et al. 2013). Although the seasonal energy conservation mechanism has been described extensively, the precise role of circadian rhythms in this process in bears is currently unknown.

Adenosine triphosphate (ATP) is the primary energy currency within the body. Quantification of ATP at intervals throughout the day can reveal how energy usage changes (Langner and Rensing 1972) and whether cellular energy management varies between seasons (Hapner Hogan et al. 2022; Hellgren 1998). Together with time-series gene transcription data, this information can provide a clearer picture of metabolic regulation at the cellular level under different seasonal conditions. Due to the seasonality of fat abundance and its importance to hibernation survival in bears, we sought to examine the relationship between circadian rhythms and cellular energetics in vitro using cultured brown bear adipose-derived fibroblasts (ADFs) obtained from white adipose tissue. To discriminate between seasonal and temperature effects, we tested cells from both active and hibernation seasons at active season (37 °C) and hibernation (34 °C) temperatures. In the current study, we measured ATP production and gene expression in ADFs sampled at frequent (3–4 h) intervals and at two different temperatures in a factorial design. We hypothesized that the amplitudes of rhythmic circadian transcripts would be reduced as would the overall transcript levels of many genes involved in metabolic processes. We also hypothesized that daily ATP production would be lower in hibernation adipose-derived fibroblasts compared to active season ADFs and that AMPK transcription would increase if ATP levels were reduced in hibernation. Finally, we expected that some transcripts would be affected by temperature alone. Together, the results of these studies bring us closer to understanding the relationship between circadian rhythms and cellular energetics in a heterothermic species.

Methods

Animals and facilities

Brown bears ($N = 1$–6) of both sexes and ranging in age from 7 to 21 years at the time of the study were used in all experiments. Bears were housed at the Washington State University Bear Research, Education, and Conservation Center in Pullman, WA. Animals were housed according to the American Society of Mammalogists guidelines (Sikes and Gannon 2011) and the Bear Care and Colony Health Standard Operating Procedures (ASAF #6468). All protocols were approved by the Washington State University Institutional Animal Care and Use Committee (ASAF #6546). Bears were fed pelleted bear feed (Mazuri Polar Bear Diet (20% protein, 25% fat, 6% fiber, and 12% moisture; formula code 5M6X; Mazuri Exotic Animal Nutrition)) and supplemented daily with fresh produce and meat or fish. Bears were fed at levels to maintain body mass in the early active season (March–July), followed by an increase during hyperphagia for mass gain (August–September); this was slowly decreased until early November when food was removed completely to induce hibernation. Bears were weighed bi-weekly between March and November to ensure that body masses were comparable to healthy wild bear populations at corresponding seasons (Keay et al. 2018).

Sample collection

Details of tissue collection methodology have been described previously (Jansen et al. 2019; Ware et al. 2013; Rigano et al. 2017). In brief, bears were anesthetized under approved protocols (ASAF #6546), blood was collected, and subcutaneous adipose biopsies were taken using a 6 mm punch biopsy (Integra-Miltex, York, PA, USA) in 2019, 2020, and 2021. All biological samples were taken between 8 and 10AM. Adipose tissue was enzymatically disrupted using Liberase ^{TM} from samples collected in May/June and January to represent summer active periods and winter hibernation, respectively. Cells were plated to expand ADFs and then cryopreserved as described in Gehring et al. (2016).

Dexamethasone synchronization

Two days before metabolic testing, adipose-derived fibroblasts from both series of experiments (RNAseq and ATP analysis) were treated with the glucocorticoid receptor agonist, dexamethasone (dex, 100 nM; Sigma, #D1756) for 15 min to synchronize their circadian phases (Balsalobre et al. 2000). Cells were then rinsed with 1X PBS three times (Ray et al. 2020). Next, PBS was replaced with normal pre-medium and the cells cultured until RNA extraction or metabolic flux analysis.

Temperature stability in incubators

To rule out that rhythms in ATP production and gene expression were caused by fluctuations in incubator temperature during sampling, we simulated our experimental protocol and subsequently monitored incubator temperatures using calibrated temperature probes (Elitech and YSI). Probes were placed in wells with DMEM medium for 24 h to allow for wells to reach incubator temperatures. The following day, adjacent well medium was removed every 4 h for 28 h, and well temperature fluctuations were monitored. Temperature was automatically recorded every 10 min for the period of 28 h.

RNAsequencing (RNAseq)

Cell culture

ADF cells obtained during the active and hibernation seasons from one WSU male brown bear ($N = 1$) were grown in 24 well plates essentially as described in (Gehring et al. 2016) with a modification of using two culture temperatures (active season Tb—37 °C and average hibernation Tb—34 °C; Fig. 1). Experimental conditions are hereafter referred to as active cells at 37 °C (A37), active cells at 34ºC (A34), hibernation cells at 37 °C (H37), and hibernation cells at 34 °C (H34). Briefly, cells were grown in preadipocyte medium containing 89% DMEM/F-12 containing GlutaMAX^{TM} (Life technologies, Carlsbad, CA, USA, #10565), 10% corresponding season and pooled serum from all bears, and 1% 100 × antibiotic/antimycotic (Sigma) with complete medium changes after the first 24 h, and then one-half change every 48 h until cells reached confluency. Cells were synchronized with dexamethasone using the same protocol as outlined below (Ray et al. 2020).

RNA extraction

Samples from individual wells from both seasons (active, hibernation) and culture temperatures (34 °C, 37 °C) were collected over the course of 72 h at three-hour intervals resulting in a total of 96 samples. Synchronized ADF's were lysed using Qiazol (Qiagen) reagent and lysates immediately stored at −80 °C until processed. Samples were processed by thawing and extraction using the manufacturers protocol (miRNeasy micro kit for cell culture; Qiagen) with a

modification using chloroform extraction as has been done previously (Jansen et al. 2019; Saxton et al. 2022). The aqueous phase was removed, and the subsequent RNA purification steps performed using an automated column extraction protocol with a Qiacube (Qiagen). Final RNA solutions were analyzed for yield and quality with a NanoDrop spectrophotometer (NanoDrop). Of the 96 samples, 3 were dropped following sequencing due to low RNA integrity number (RIN) scores. The three samples were the last of the entire time series to be extracted (66, 69, and 72 h; all from H34). Once quality control was performed, samples were frozen at −80 °C until library preparation and RNA sequencing (RNAseq).

Library preparation and sequencing

For RNAseq, strand-specific, paired-end libraries were prepared from the total RNA by ribosomal depletion using the Ribo-Zero rRNA removal kit (Illumina), followed by the TruSeq stranded total RNAseq kit (Illumina) according to the manufacturer's instructions. Next, 100 base pair (bp) paired-end reads were sequenced using a Illumina NovaSeq 6000 system according to the manufacturer's instructions.

Mapping and expression

Raw RNAseq read quality was assessed with FastQC (version 0.11.9; Andrews 2010) and subsequently trimmed with Trim Galore! (version 2.10; Krueger 2014). Trimmed reads were mapped to the most recent chromosome-level brown bear genome assembly (GCF_023065955.1_UrsArc1.0; Armstrong et al. 2022), using STAR (version 2.7.6a; Dobin et al. 2012). We used featureCounts (version 2.0.3.; Liao et al. 2013) to estimate the number of reads mapping to each gene in the reference annotation set of the brown bear genome. Gene expression was normalized as transcripts per million using base R. Lastly, principal component analysis was used to visualize key differences in expression data using edgeR (Robinson et al. 2009).

Circadian analysis

The robustness of the chosen experimental sampling interval and duration, i.e., 3-h intervals for 72 h for our RNAseq experiment, was compared to synthetic data generated within TimeTrial for transcriptomic time-series data (Ness-Cohn et al. 2020). We selected the following TimeTrial parameters to confirm the robustness of our approach: replicates = 1 vs. 2, length = 72 h, interval = 2 vs 4 h (3 h is not an option), noise level = 0.1, and methods = Arser_Avg vs. JTK_Cycle. The resulting accuracy to define the 11 different types of patterns in the data set ranged from 46.4–100% depending on method, replicate number, and sampling interval. A "sin" (sinusoidal; i.e., pure oscillatory pattern) pattern was correctly classified in 100% of runs regardless of replicate number. Next, circadian parameters (period, phase, and amplitude) for each transcript were determined using MetaCycle (version 1.2.0; Wu et al. 2016) that incorporates the use of JTK (Hughes et al. 2010), LS (Ruf 1999), and ARSER programs. The stringency of the programs is as follows in order from most stringent to least; LS, MetaCycle, JTK, and ARSER. Due to the three missing time point values in H34, we supplemented missing data with the expression values of identical time points from day 1. We applied the meta2d function using default parameters except weightedPerPha was set to TRUE. Genes were considered rhythmic if $p \leq 0.05$. Our initial analysis included all expressed genes and focused on searching for circadian periods between 18 and 27 h, a second analysis included ultradian (less than a day) periodicities (i.e., 9 to 17 h), and a third analysis removed genes expressed at very low levels (i.e., average expression across time points < 1 transcripts per million, tpm, in a given treatment) to rule out false positives.

E-box motif scanning

To assess whether the promoters of genes with rhythmic expression in each treatment were enriched for the presence of the E-box binding site motif, we conducted binding site enrichment analysis with CiiiDER (version 0.9; Gearing et al. 2019) using the E-BOX/CLOCK binding site position weight matrix from the JASPAR database (Motif ID: MA0819.1; Castro-Mondragon et al. 2022). Promoters were defined as the 500 bp region upstream of the transcription start site of each gene (Korkuc et al. 2013). For each treatment, we used the promoters of all rhythmic genes as the foreground, and promoters of non-rhythmic genes with non-zero expression (i.e., normalize counts greater than zero in at least one time point) as the background. Enrichment analysis in CiiiDER was run with default parameters, and results with a gene coverage p-value < 0.05 and log2 enrichment value > 0 were considered to be enriched for E-box motifs relative to the background.

Weighted gene co-expression networks

To identify modules of co-expressed genes, we split the samples by season and temperature. We conducted a weighted gene co-expression network analysis (WGCNA) on all expressed genes meeting the expression cutoff (i.e., genes with average expression across time points < 1 tpm in a given treatment were removed) using the R package WGCNA (version 1.71; Langfelder and Horvath 2008, 2012) as described in Jansen et al. (2019). Before constructing the networks, we determined a soft thresholding power of 12, which was identified using pickSoftThreshold in the WGCNA package

in R, such that the model fitting index $R^2 > 0.9$. To identify signed networks, the blockwise Modules function in the WGCNA package in R was used with networkType = signed, TOM Type = signed, min ModuleSize = 30, reassign Threshold = 0, merge CutHeight = 0.25, max BlockSize = 10,000, and all other default options. Modules that were found to be correlated with one or more experimental traits (season and temperature; > 0.5; p value < 0.05) were analyzed for overrepresentation of gene ontology (GO) terms as described below.

Overrepresentation analysis

Rhythmic gene groups and modules highly correlative with season or temperature were analyzed for overrepresentation analysis using WebGestalt (version 2019; Wang et al. 2017). Gene sets were compared to the human genome (GCA_000001405.29), and the search was limited to those GO terms with an FDR < 0.05.

Cluster analysis

Mfuzz (Bioconductor version 3.16; Kumar and Futschik 2007) package was utilized to perform an unsupervised learning of our time-series data and soft clustering to identify clusters with similar (temporal) traits. We performed this analysis on expression data for both rhythmic MetaCycle genes containing an E-box and all MetaCycle rhythmic genes. All conditions were grouped into 10 separate clusters as calculated using Dmin, which calculates minimum centroid distance between clusters. These clusters were confirmed with a post hoc correlation test between centroids with a limit of 0.85 between clusters. Gene lists were then extracted, and overrepresentation analysis was performed on individual clusters.

Daily ATP production rate

Cell culture

ADFs were obtained from brown bears ($N = 6$) during both active and hibernation seasons as described above (Fig. 1). Cells were grown in 8-well XFp Seahorse plates (Agilent, #103725–100) at 37 °C (active) or 34 °C (hibernation) in 5% CO_2 as described in (Hapner Hogan et al. 2022). Briefly, cells were grown in pre-adipocyte medium (pre-medium) containing 89% DMEM/F-12 with GlutaMAX™ (Life technologies, Carlsbad, CA, USA, #10565), 10% matching season bear serum pooled from the six bears used for study to reduce individual variation, and 1% 100 × antibiotic/antimycotic (Sigma, #15240) (final concentrations 100 units/ml penicillin, 100 mg/ml streptomycin, and 0.25 mg/ml amphotericin B), and 5.5 mM glucose. Culture medium was changed completely 24 h after plating and then every 48 h with one-half volume until cells reached confluency.

Metabolic flux analysis overview

A Seahorse XFp Extracellular Flux Analyzer (Agilent Technologies, Inc., Santa Clara, CA, USA) was used to directly measure extracellular acidification rate (ECAR) and oxygen consumption (OCR). ECAR was then converted to proton efflux rate (PER) to more accurately reflect acidification by anaerobic respiration and lactate production. PER was calculated using the following formula:

$$\begin{aligned} \mathrm{PER} &= ECAR\,(mpH/\min/\mu g\,protein) \\ &\times buffer\,factor\,(mmol/L/pH) \\ &\times geometric\,well\,volume\,(\mu L) \\ &\times Kvol\,(constant) \end{aligned}$$

A buffer factor of 2.3 was used as previously determined by our laboratory (Hapner Hogan et al. 2022). The calculated PER and OCR were then used to calculate rates of glycolysis, OXPHOS, and ATP production following injection of specific inhibitors as described below (Mookerjee et al. 2016, 2017).

For the quantification of ATP derived from OXPHOS, oligomycin was injected. Oligomycin inhibits ATP synthase (complex V) and ATP production due to OXPHOS. This reduction of oxygen consumption was deducted from basal OCR to estimate ATP_{mito}. Then, injection of the combination of rotenone and antimycin A which inhibits ETC complexes I and III, respectively, inhibits proton flow within the ETC. This manipulation along with the appropriate buffer factor of the medium, allowed ATP production from glycolysis (ATP_{glyco}) to be estimated using the following formula:

$$\mathrm{ATP}_{glyco} = glucose + 2\,ADP + 2\,\Pi \rightarrow 2\,lactate + 2\,ATP$$

based on the conversion of glucose to lactate (Mookerjee et al. 2017). ATP_{oxphos} was determined using the following formula:

$$\begin{aligned} \mathrm{ATP}_{oxphos} &= ATP - coupled\,OCR\,(OCRATP \\ &= OCR_{total} - OCR_{oligomycin}). \end{aligned}$$

where OCR_{total} is defined as the basal OCR or OCR prior to oligomycin injections and $OCR_{oligomycin}$ is the OCR after injection. ATP_{oxphos} was then calculated by multiplying OCRATP by two (2) to convert oxygen molecules to atoms of oxygen and then by the average phosphate-to-oxygen (P/O) ratio of 2.75 to account for the oxidation of substrates

in the medium during the assay (Mookerjee et al. 2017). The total ATP was determined by adding ATP_{glyco} and ATP_{oxphos} (Supplemental Fig. 2).

Daily changes in ATP production

Seahorse culture plates were prepared according to Hapner Hogan et al. 2022 with minor changes as follows: the day before the assays Agilent Seahorse XFp Sensor Cartridges (Agilent Technologies) were hydrated with Seahorse XF Calibrant solution for at least 12 h (Agilent Technologies, 103059–000). The Seahorse XFp Extracellular Flux Analyzer was turned on and allowed to warm to the appropriate assay temperature for at least 24 h prior to assay. On the day of the assay, cells were incubated in a non-CO2 incubator at 37 °C or 34 °C for 1 h in assay-specific medium. Assay medium constituents and drugs used are assay-specific and were always reconstituted in Seahorse XF DMEM Medium (starting pH 7.4, Agilent Technologies, 103575–100). Glucose concentration for assay medium was altered from manufacturer's recommendation to 5.5 mM to match the fasting concentrations measured in bears at WSU (Hapner Hogan et al. 2022). Oligomycin a complex V inhibitor and rotenone/antimycin A, complex I and III inhibitors were part of real-time ATP rate assay kits designed specifically for use in the Seahorse (Agilent, #103591–100). ATP rate determinations were made in independent plates every 4 h for a period of 28 h at both temperatures. All results were normalized to protein (µg) per well using BCA (bichoncinic acid) kits (Sigma).

Data analysis

Raw Seahorse OCR and ECAR data were analyzed using Wave software. ATP production was then estimated using the Seahorse ATP rate conversion formulas (Agilent). Protein-normalized data were analyzed using R statistical software. Three-way ANOVAs with time, temperature, and season as main factors and individual animal as a random effect were analyzed for statistical significance using base R (The R project for Statistical Computing 2023), lme4 (Bates et al. 2015), and emmeans. The cutoff for statistical significance was an alpha of 0.05. Figures were generated using R, BioRender (BioRender.com), or GraphPad Prism (v9.0, GraphPad Software, San Diego, CA USA).

Results

Rhythmic transcription is present in all experimental conditions

Genes with significant rhythmic expression ($p < 0.05$) were identified in all conditions (A37, A34, H37, and H34) using both MetaCycle and ARSER (Fig. 2, Table 1, 2, Supplemental Fig. 3, 4, 5). Consistent with other brown bear hibernation studies, there were also numerous unique *rhythmic* genes between active and hibernation season conditions at both temperatures (Fig. 2). Multiple genes known to be involved in circadian function and metabolism showed rhythmic expression in one or more treatments. A circadian gene, *PER2,* and a clock-controlled mitochondrial gene coding for cytochrome c proteins, *COX1*, were rhythmically expressed in all four experimental conditions (Table 1). Several other circadian genes: *NR1D2* (A37, A34, H34), *CRY1* (A37, A34), *CRY2* (A37, H34), *ARNTL* (*BMAL11*) (A37, H37), *PER1* (A34, H34), and *PER3* (H34) were confirmed to be rhythmic under various experimental conditions (Table 1). Several metabolic genes were also found to be rhythmic in the active and hibernation season, most notably, *SIRT1* (A37, H34), the *PRKA* (*AMPK*) family of genes (A37, A34, H37, H34), *COX 2* (A37, H37, H34), *ATP6* (H37, H34), *ATP8* (H37, H34), *ND2* (A37, A34, H34), *ND3* (H34), and *ND1* (A37, H34) (Table 1). Several different ranges of rhythmicities were used to provide an accurate representation of the number of rhythmic genes present. Depending on the analysis, 1,800 to 10,000 genes were rhythmic (Table 2). Analysis of an incubator sampling confirmed no significant time effect due to fluctuation in temperature that would lead to masking of circadian rhythms (34 °C: *ANOVA*, $p = 0.1657$; 37 °C: *ANOVA,* $p = 0.832$; Supplemental Fig. 6).

The *PRKA* (AMPK) family of genes except for the beta subunit had significantly higher mean expression (*t*-test, $p < 0.05$) and higher amplitudes in H34 as opposed to A37 (Supplemental Table 1), while *SIRT1* had significantly lower mean expression and a lower amplitude in H34 (*t*-test, < 0.0001). *NAMPT,* and *PGC1 α* had significantly lower mean expression (*t*-test, $p < 0.005$) in H37 and lower amplitudes in H34 in contrast to A37. The core circadian genes generally had significantly lower mean expression except for *CRY2* and *CLOCK* in H34 (*t*-test, $p < 0.0001, = 0.001$), with a similar pattern (lower in H34) for amplitude (Supplemental Table 2). Mitochondrial gene mean expression (Supplemental Table 3) was generally significantly decreased or unaffected (*t*-test, $p < 0.05$), and amplitudes were generally elevated (Supplemental Table 3). Circadian period was significantly affected by temperature alone (*two-way ANOVA*, $F_{1,12176} = 425.19$,

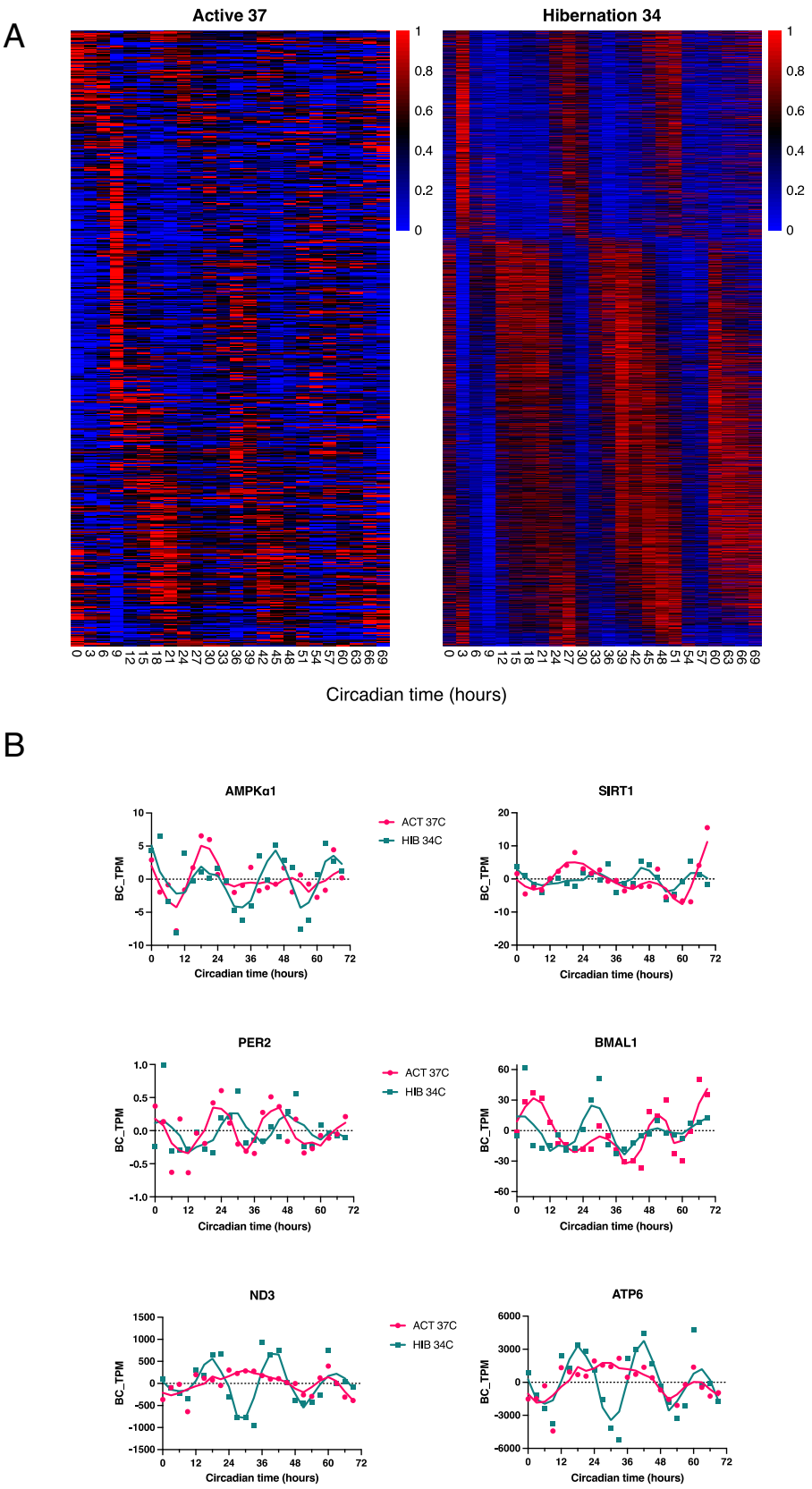

Fig. 2 **A** Heat maps showing expression values for MetaCycle rhythmic genes aligned by peak phase and for matched season and temperature conditions: A37 and H34. Each row represents an individual gene. The data are plotted across the 72-h sampling period. In order from left to right, each condition contains 928, 527, 882, and 3318 transcripts, respectively. **B** Individual expression profiles for two metabolic, circadian, and mitochondria genes in conditions with matched season and temperature and sampled every 3 h. Individual points represent baseline corrected TPM (BC_TPM) calculated as the difference: raw TPM value minus baseline) using GraphPad Prism (v. 9 for Mac). Baseline TPM was assumed to be linear with time. For the smoothed lines, a three-point moving average followed by a second order polynomial was used (Prism)

Table 1 List of genes that exhibited rhythmic transcription across experimental conditions

	A37	A34	H37	H34
Circadian	*ARTNL*	*CRY1*	*ARNTL**	*CRY2*
	*CLOCK**	*NR1D2*	*PER2*	*NR1D2*
	CRY1	*PER1*	*NR1D1**	*PER1*
	*CRY2**	*PER2*		*PER2*
	NR1D1	*CRY1*		*PER3*
	NR1D2			
	PER2			
Metabolism	*ATP8*	*COX1*	*ATP6*	*ATP6*
	COX1	*ND2*	*ATP8*	*ATP8*
	COX2	*ND5*	*COX1*	*COX1*
	CYTB	*ND6*	*COX2*	*COX2*
	NAMPT	*PRKAA1*	*PRKAA1*	*COX3*
	ND1	*PRKAA2*	*PRKAA2*	*CYTB*
	ND2		*PRKAG1*	*NAMPT*
	ND4		*PRKAG2*	*ND1*
	ND4L			*ND2*
	ND5			*ND3*
	ND6			*ND3*
	PRKAG1			*ND4*
	SIRT1			*ND4L*
				ND5
				ND6
				PGC1a
				PRKAA1
				PRKAA2
				PRKAG2
				SIRT1

Circadian clock genes are those that have functions in regulating the core circadian clock via transcriptional–translational feedback loops. Metabolism genes are those involved in regulating metabolic processes, including those in the mitochondria

*Represents genes with a period less than 17 h, indicating a possible ultradian rhythm. See METHODS for additional details

Table 2 Table with the number of significant rhythmic genes (ARSER; $p < 0.05$) with various data manipulations

	A37	A34	H37	H34
No genes removed *(period 18-27)*	2044	2604	1894	5639
No genes removed *(period 9-27)*	7511	7348	7889	10893
Lowly expressed genes removed *(period 9-27)*	5010	4331	4194	7401

Row 1 is the initial search with no lowly expressed genes (< 1 tpm) removed and a period setting of 18 to 27 h. Row 2 is similar but with a lower period setting to examine the presence of ultradian expressed genes. Row three has the same period settings as row 2 and removes the lowly expressed genes with a mean average of less than 1. See METHODS for additional details

$p = < 0.0001$), season alone (*Two-way ANOVA*, $F_{1,12176} = 37.67$, $p = < 0.0001$), and temperature and season (*two-way ANOVA*, $F_{1,12176} = 74.851$, $p = < 0.0001$). Representative circadian and metabolic gene rhythm amplitudes for each experimental condition are shown in Supplemental Fig. 7.

E-box motifs are present in the promoter regions of rhythmic genes

We tested whether the promoters of genes with rhythmic expression were enriched for the presence of E-box binding site motifs using CiiiDER. Rhythmic gene promoters were enriched for the presence of E-box motifs in treatments A34, H34, and H37 ($p < 0.05$; Supplemental Table 4). Somewhat surprisingly, E-box motifs were found to be significantly depleted in promoters in the A37 treatment ($p = 0.0308$, $\log_2$ enrichment = −0.213).

Weighted gene co-expression network analysis

All genes were assigned co-expression modules using WGCNA, and module eigengenes were correlated with experimental conditions. We identified 36 modules of co-expressed genes, of which 4 and 7 were significantly correlated with season and temperature, respectively (Supplemental Fig. 8, Supplemental Table 5). Additionally, there is a module for genes that were unable to be unassigned to other modules. Modules affected by temperature were enriched for GO terms related to positive regulation of gene expression, autophagy, and protein modification, and modules affected by season were involved in mitochondrial gene expression and protein folding.

Gene ontology characterization of rhythmic genes

Genes that were considered rhythmic with ARSER analysis ($p < 0.05$) were assessed for overrepresented gene ontology (GO) terms in all four conditions. Protein localization and DNA/RNA synthesis were significantly over-represented (FDR < 0.05) in rhythmic genes in all four conditions (Supplemental Table 6, 7). A37 was over-represented for cell cycle processes and DNA repair, while H34 was over-represented for terms related to metabolism. In the H37 and A34, protein localization and translation were the processes that were most over-represented (Supplemental Table 6, 7).

Season, temperature, and time of day affect cellular metabolic function

Basal OCR exhibited significant increases in the active season (*ANOVA*, $F_{1,155} = 6.538$, $p = 0.0115$), at the higher temperature (*ANOVA*, $F_{1,155} = 4.492$, $p = 0.0356$) and interaction

between temperature and time (*ANOVA*, $F_{1,155} = 20.310$, $p = < 0.0001$). Similarly, basal ECAR exhibited significant increases in the active season (*ANOVA*, $F_{1,155} = 7.971$, $p = 0.0054$), temperature (*ANOVA*, $F_{1,155} = 18.633$, $p < 0.0001$), and time (*ANOVA*, $F_{1,155} = 4.555$, $p = 0.0344$). The interaction between temperature and time for basal ECAR was significant (*ANOVA*, $F_{1,155} = 17.661$, $p < 0.0001$). Time and the three-way interaction between season, temperature, and time were not significantly affected. The total ATP exhibited a significant interaction between season and time (*ANOVA*, $F_{1,155} = 4.296$, $p = 0.0399$) and temperature and time (*ANOVA*, $F_{1,155} = 21.756$, $p = < 0.0001$) (Fig. 3, Supplemental Fig. 9). The mean total ATP production was higher overall in the active season cells (A37) versus the hibernation season (H34) cells (Fig. 3), which is consistent with previous studies (Hapner Hogan et al. 2022). Glycolysis rates were significantly lower in the cells grown at 37 °C than those grown in 34 °C (*ANOVA*, $F_{1,184} = 41.2414$, $p = < 0.0001$; Supplemental Table 9), and OXPHOS was significantly increased in hibernation (*ANOVA*, $F_{1,184} = 4.9547$, $p = 0.027234$). Rates of glycolysis rates ranged from 0–25% in all conditions, with the majority of total ATP derived from OXPHOS (75–100%).

Discussion

This study aimed to elucidate the relationship between energy metabolism, gene expression, body temperature, and circadian rhythms in brown bears in vitro using a cell culture system. The current findings expand on our previous work demonstrating that bears continue to express circadian rhythms throughout dormancy (Jansen et al. 2016; Ware et al. 2020, 2013). Importantly, we observed a clear relationship between mitochondrial ATP production and circadian transcript rhythms during hibernation, highlighting the distinct difference between bears and other hibernating mammals (Revel et al. 2007; Williams et al. 2017). We now report that mitochondrial metabolism and transcription are regulated temporally in ADF's obtained from hibernating

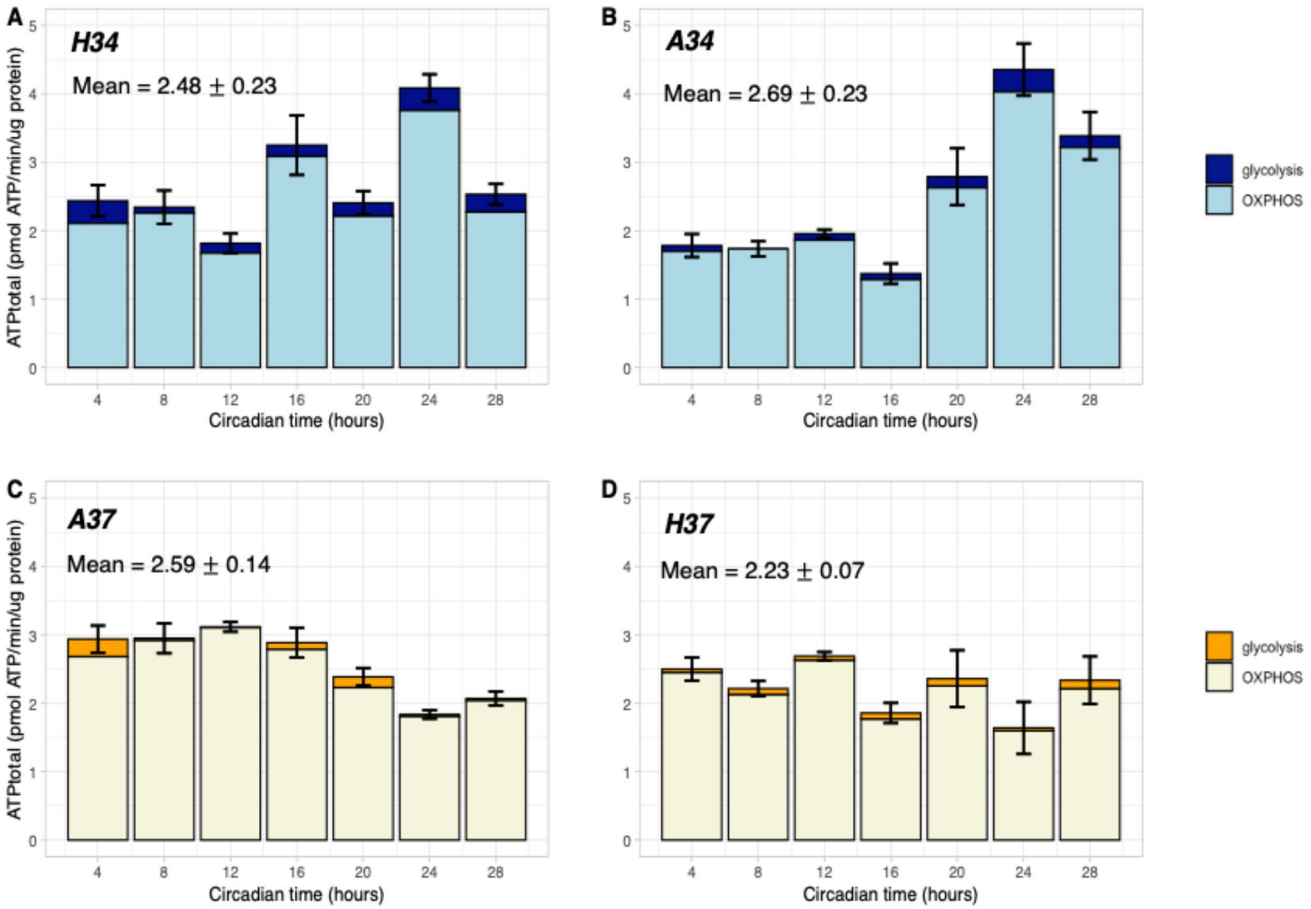

Fig. 3 Stacked bar plots showing mean (±SEM) ATP production in samples collected at four-hour intervals in all experimental conditions over a period of 28 h. Time is representative of circadian time. Mean (±SEM) daily ATP production is included in each panel. Darker shading indicates ATP production due to glycolysis, and lighter colors indicate ATP production due to oxidative phosphorylation (OXPHOS)

brown bear white adipose tissue providing a mechanistic link between these two processes. Intriguingly, we also observed that lower temperature (34ºC) delayed the peak of ATP production, along with a small, but significant reduction in ATP production. Together, the linking of circadian rhythms and ATP production in hibernation cells strongly suggests an energy conserving mechanism. It is well established that disruption of circadian rhythms in species from mice to humans results in metabolic disturbances (Bass and Takahashi 2010). Thus, maintaining rhythms may ultimately be one of the mechanisms whereby bears prevent the development of metabolic diseases. Importantly, these rhythms do not require a light–dark cycle to drive them, hence the benefit of an endogenously generated rhythm. In addition, by modulating the amplitude of the circadian rhythm of the energy-sensing gene, *AMPK*, along with *SIRT1*, bear cells may invoke a cellular homeostatic mechanism to lower their metabolic rate at elevated body temperature which warrants further study.

Circadian gene expression persists in hibernation

Diel cycles (exactly 24 h) are to be expected in active and hibernating brown bears subjected to day-night cycles (Ware et al. 2013; Jansen et al. 2016; Thiel et al. 2022) due to entrainment by the light–dark cycle; however, determining their circadian genesis, with a requisite period that is *different* from 24 h, requires constant environmental conditions (Vitaterna et al. 2001). An in vitro system provides an ideal platform to confirm this. We found thousands of genes were transcribed rhythmically in all season and temperature combinations. In support of previous findings (Zhang et al. 2014; Ptitsyn and Gimble 2011; Ray et al. 2020), we found that approximately 10–45% of genes were rhythmic depending on the experimental conditions. Specifically, genes associated with the core circadian clock TTFL—*NR1D2*, *Per2*, and *CRY2* were rhythmic in both seasons providing further evidence that the circadian system is continuing to function during hibernation. Furthermore, we found that period was significantly shortened at a lower temperature and between seasons. This finding supports previous work in rat fibroblasts which revealed that colder temperatures sped up peripheral clocks and in turn shortened period (Izumo et al. 2003). Our data are reflective of ADF's within adipose tissue; however, coupled with data from mature adipocytes (unpublished data) and behavioral and Tb rhythms (Jansen et al. 2016), it is evident that circadian rhythms remain an important component of hibernating bear physiology. Based on our ATP results, one can hypothesize that maintaining a rhythm in cells allows metabolism to function more efficiently, even at lower temperatures. This would be required during hibernation in bears when nutrient intake is not occurring. Furthermore, given the reduction in circadian rhythm amplitude (present study and Jansen et al. 2016) coincident with the lowered metabolic rate, it is also plausible that the two are causally related, although this remains to be tested directly.

Genes involved in metabolism express circadian rhythms in hibernation

Several known metabolic genes that directly interact with the circadian system or are driven by the clock were found to be rhythmic in both conditions with matched season and temperature (H34 and A37; Fig. 2). For example, *PRKA* (*AMPK*) is an energy-sensing gene that directly impacts the circadian system by enhancing the degradation of CRY proteins in response to elevated AMP/ADP:ATP ratios (Jordan and Lamia et al. 2013). Similarly, *SIRT1* and *NAMPT* both interact with the circadian system via their relationships with NAD^+. *NAMPT* is the rate-limiting enzyme for production of NAD^+, and *SIRT1* induces transcription of *CLOCK* when NAD^+ levels are elevated which directly leads to *BMAL1* transcription (Ramsey et al. 2009). Additionally, *SIRT1* has a role in stabilizing *PER2*, which was also rhythmic in active and hibernation seasons (Asher et al. 2008). Inhibition of *NAMPT* promotes transcription of *PER2* by preventing the suppression of the *CLOCK/BMAL1* heterodimer via *SIRT1* (Ramsey et al. 2009). Together, these genes play a role in connecting nutrition and metabolism with circadian timing to potentially optimize energetic processes. Additionally, *PGC1 α* regulates metabolism through the circadian system by activating nuclear receptors that induce expression of *BMAL1* and *NR1D2* (Liu et al. 2007), and both were found to be rhythmic in several conditions in the current study. In concordance with our previous studies (Vella et al. 2020), *PGC1 α* transcript levels were decreased in hibernation. Importantly, we observed that those genes that interact with NAD^+ to directly connect clocks to OXPHOS also led to rhythmic ATP production. Because these genes were rhythmic both in the active season and hibernation, it suggests that circadian regulation of metabolism, especially its timing, is important at all times of year.

Many of the rhythmically expressed genes encode for proteins of the ETC. This was confirmed by a co-expression module that was associated directly with mitochondrial gene expression (Supplemental Table 5). Rhythmic active cells (A37 and A34) were over-represented for cell growth and division, whereas hibernation type cells (H37 and H34) were over-represented for metabolism and protein synthesis (Supplemental Table 6, 7). This difference in the families of genes being rhythmically transcribed could represent a novel adaption of the circadian system to nutrient deficit (Asher and Sassone-Corsi 2015; Bass and Takahashi 2010). Numerous cycling mitochondrial genes revealed in the present study are essential for ETC function (Tzagoloff and

Macino 1979). For example, *ATP6* encodes the F_0 functional domain of ATP synthase (or complex V) of the OXPHOS chain and transfers energy derived from the proton gradient and is responsible for the phosphorylation of ADP to ATP in F_1 (Jonckheere et al. 2012). Likewise, those genes coding for NADH dehydrogenases (*ND1-ND6*) and cytochrome c and b oxidase (*COX1-2, CYTB*) catalyze the transfer of electrons from NADH down the transport chain which ultimately leads to the creation of the proton gradient that drives ATP synthase (Weinrich et al. 2019). Rhythmic expression of these mitochondrial genes is consistent with ATP levels changing in a time-dependent fashion (Figs. 2, 3). However, since these genes do not contain E-boxes in their promoters, circadian regulation is indirect via other clock-controlled genes.

Mitochondrial function is highly rhythmic in hibernation

Both season and temperature interacted separately on the time of day that the maximal total ATP was produced. The temporal separation of metabolic processes is common across taxa from cyanobacteria (Stöckel et al. 2008) to mice (Hodge et al. 2015) for the purpose of timing energetic events to the ideal times of day or separating cellular processes that cannot occur simultaneously (Wang and Stephanie 2015). The present findings support the hypothesis that temporal (circadian) regulation of mitochondrial respiration and production of ATP provides an adaptive advantage in timing energy production to ideal environmental conditions (Schmitt et al. 2018). The timing of ATP production to later in the day at lower temperature most likely is due to a direct effect of temperature on enzyme kinetics because mitochondrial enzymes are not temperature compensated (Battersby and Moyes 1998). Nevertheless, the relatively small reduction in the total ATP indicates that timing of ATP production, rather than amount of ATP, may have a greater role to play. This is perhaps not surprising because highly seasonal animals must still maximize energetic efficiency daily during extended periods without food resources (Körtner and Geiser 2000). Furthermore, the longer cycle length of hibernating bears held under constant conditions (Jansen et al. 2016) such as those in culture, would be expected to be delayed, rather than advanced. Thus, the demonstrated interactions between metabolic and circadian systems in an animal expressing shallow torpor expand our understanding of these vital processes under the extremes of hibernation (de Goede et al. 2018; Bellet et al. 2011; Rutter et al. 2002).

Both season and temperature have effects on gene expression and ATP production

Due to the factorial nature of our experiment, we were able to separate changes in transcription and ATP production due to season and temperature. ADFs performed metabolically as expected based on previous bear cell culture work (Hapner Hogan et al. 2022), with ATP production being slightly but significantly, lower in the hibernation condition (H34) cells vs. the active condition (A37). Additionally, ATP produced from glycolytic pathways in all conditions only attributed ~ 5% of total ATP production, while OXPHOS contributed to the majority of ATP production (~ 95%). This delegation of processes can be explained by the 4 × greater ATP yield produced through OXPHOS as opposed to glycolysis (Mookerjee et al. 2016). Hibernating bears must conserve valuable stored carbohydrates and tend to rely more heavily on lipid metabolism while they remain in a fasted state (Storey 1997; Rigano et al. 2017; Barboza et al. 1997; Farley and Robbins 1995). These distinct seasonal differences are also highlighted in the transcriptomic data and are consistent with previous studies (Fig. 4; Supplemental Fig. 10; Jansen et al. 2016, 2019, Saxton et al. 2022; Hapner Hogan et al. 2022; Ware et al. 2013). However, the relatively small reduction in ATP production and increase in glycolytic function in H34 was surprising. The most likely explanation is that the current study used ADFs, while that of Hapner Hogan et al. (2022) used adipocytes. The much larger lipid content in the latter would be consistent with a shift in energetic usage to lipid based, rather than glycolytic.

Our experiments revealed temperature effects on the time of day that peak ATP levels were produced. Adipose-derived fibroblasts grown at 37 °C exhibited a peak in ATP production at 8 h, corresponding to earlier in the day, while the 34 °C cells had highest production at 24 h, corresponding to later in the day. In accordance with this pattern, all mitochondrial genes had delayed peaks in gene transcription in (H34) as opposed to (A37). It is worth noting that the precise timing of transcriptional events in relation to actual energetic outputs (i.e., OCR and PER) is offset in time based upon how far upstream transcriptional events are taking place. Furthermore, *ND3*, *ND5*, *ATP6*, *ATP8*, and *COX2* transcript levels were significantly impacted by temperature alone, whereas most circadian and clock-controlled metabolism genes had exhibited a seasonal or a season by temperature interaction. The delay in peak levels of transcripts involved in State 3 respiration (increased ADP) is consistent in the delay in AMPK expression and reductions in ATP production. Overall, it appears the regulation of hibernating bear ADF respiration is like other hibernating species (Barger et al. 2003). Moreover, based on the increased amplitude of most transcript rhythms in the ETC, it appears that bear

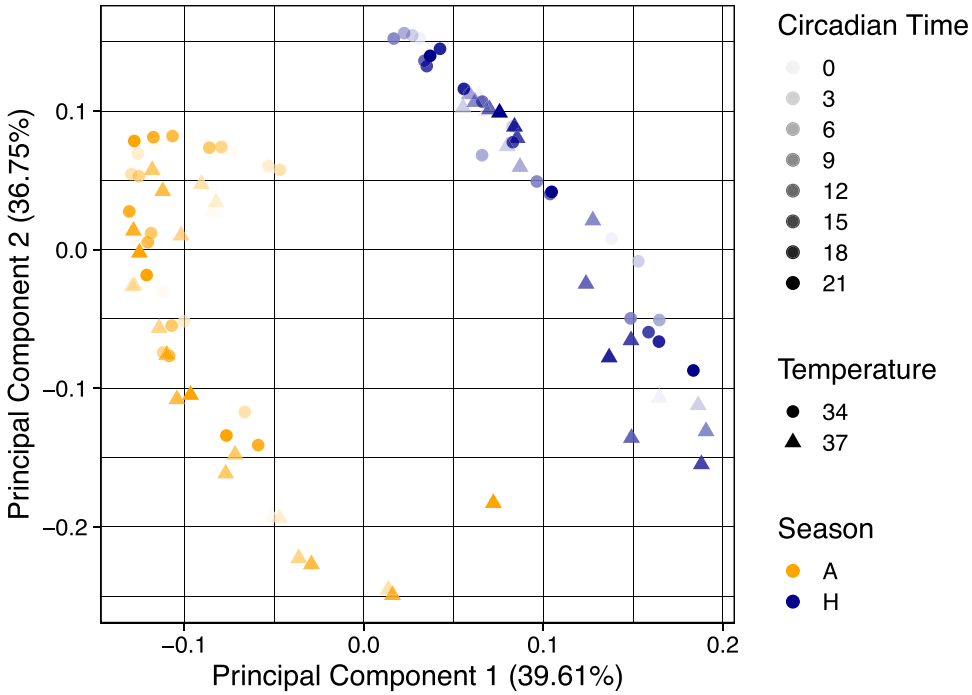

Fig. 4 Principal component plot of gene expression across four experimental conditions. Each point represents gene expression at a given time point, and samples were taken every 3 h for 72 h. Dot shading is indicative of the circadian time of day when a sample was taken. Darker colors are later in the circadian day, while lighter colors are earlier

ADF mitochondria are similar to other species where mitochondrial enzyme activity is *increased* under *lower* temperatures (Guderley and St.-Pierre 2002). This conjecture remains to be verified in experiments where the temperature is lowered during an experiment and ATP rates are monitored. Taken together, the present findings highlight a time-dependent influence on OXPHOS that is influenced by relatively modest decreases in body temperature accompanying the hibernation season phenotype of bears. This also adds a new dimension to the complexity of whole cell metabolism under various seasonal conditions.

Cost: benefit relationship of circadian rhythms in hibernation

Previous work has shown that cycling transcripts are more energetically costly to produce compared to those that do not cycle (Wang and Stephanie 2015). This suggests that the energetic benefits obtained by temporally isolating metabolic processes in hibernation must outweigh the cost of being rhythmic. Our original hypothesis proposed that rhythm amplitudes would be lower in the hibernation season and at lower temperatures compared to active season, but that average expression would not change. Indeed, we confirmed that the amplitudes and mean expression of several circadian genes *BMAL1*, *CRY* , and *PER*, were reduced, but that mitochondrial gene expression and amplitudes tended to be elevated in H34 (Supplemental Fig. 7). The increase in the mitochondrial amplitude in concert with no change in mean expression suggests that adjusting transcript rhythm amplitude may allow hibernating cells to counter the overall cost of cycling gene expression.

Conclusions

We have provided further evidence that brown bears retain cellular circadian and metabolic rhythms during hibernation. Importantly, we have elucidated a relationship between temporal partitioning of mitochondrial ATP production and the circadian system that, together, suggest the internal clock remains inextricably linked with metabolic processes in dormancy. We have also uncovered a strong temperature effect on daily energy production and one that occurred at a relatively modest lower temperature. This information brings us one step closer to completely understanding hibernation energy regulation that could have direct implications to our understanding of hibernation evolution and the management of metabolic pathologies.

Limitations and considerations

We note that the present findings are based on RNA generated from cells of a single individual. While subsequent studies with increased biological replication would certainly

be valuable for further understanding the role and variation in circadian expression in hibernating bears, we are confident in the conclusions of this study for several reasons. First, TimeTrial analysis of the experimental design indicated that sine wave rhythmicity (a typical circadian waveform) could be detected with 100% confidence, even for a single individual, if the sampling frequency was less than 4 h, and our sampling was every 3 h. Second, heat maps of gene expression (Fig. 2) clearly revealed peaks and troughs of expression and varying phases. Finally, soft clustering (Supplemental Fig. 3), using an unbiased assigning of rhythmic transcripts, revealed rhythmic profiles of at least ten different varieties. The single individual we used for the RNAseq analysis, an adult male, was also used for the ATP rate experiment to preserve continuity. Another limitation is that due to the three day sampling period of this study, we were unable to identify infradian rhythms. As these studies were performed using bears in a captive setting, the conditions do not exactly mimic those found in the wild. Nevertheless, cultured cells were treated identically to eliminate external influences. The function of genes containing E-boxes was inferred, and thus, additional experiments that incorporate chromatin immunoprecipitated sequencing (ChIP-seq) or similar approaches will be needed to confirm their circadian roles.

Supplementary Information The online version contains supplementary material available at https://doi.org/10.1007/s00360-023-01513-5.

Acknowledgements This work was supported by the Bear Research and Conservation Endowment at Washington State University, National Science Foundation Office of Polar Programs Grant to JLK (award number: 2312253), and the National Science Foundation Office of Polar Programs Post-Doctoral Fellowship to BWP (award number: 2138649). We would like to thank Marina Savenkova for her technical support in the laboratory and Sascha Duttke for sequencing our RNA samples. We would also like to acknowledge and thank all the volunteers and staff at the Washington State University Bear Center, especially Brandon Evans-Hutzenbiler, Heather Keepers, Chelsea Davis, Tony Carnahan, Jessie McCleary, and Heather Havelock and the WSU Kamiak high-performance computing cluster that make this research possible. The authors are also thankful to the two anonymous reviewers for the helpful comments.

Authors contribution HTJ and CTR obtained funding; EPV, JLK, and HTJ designed the study; HTJ, CTR, and EPV performed the blood and tissue sampling; EPV and HTJ performed the metabolic flux analyses, and transcription experiments; EPV, JLK, BWP, and HTJ analyzed the data; the first draft of the manuscript was written by EPV, and all authors read and approved the final manuscript.

Data availability All newly generated circadian RNAseq data are available on NCBI under BioProject (PRJNA986183). Code is available on GitHub at (https://github.com/Jansenht/Vincent_JCPB_ursus).

Declarations

Conflict of interest The authors declare no conflicts of interest due to economic or commercial relationships.

References

Andrews S (2010) FastQC: a quality control tool for high throughput sequence data

Armstrong EE, Perry BW, Huang Y, Garimella KV, Jansen HT, Robbins CT, Tucker NR, Kelley JL (2022) A Beary good genome: haplotype-resolved, chromosome-level assembly of the brown bear (Ursus arctos). Genome Biol Evol 14(9):evac125. https://doi.org/10.1093/gbe/evac125.2022

Aschoff J (1960) Exogenous and endogenous components in circadian rhythms. Cold Spring Harb Symp Quant Biol 25:11–28. https://doi.org/10.1101/sqb.1960.025.01.004

Asher G, Sassone-Corsi P (2015) Time for food: the intimate interplay between nutrition, metabolism, and the circadian clock. Cell 161:84–92. https://doi.org/10.1016/j.cell.2015.03.015

Asher G, Gatfield D, Stratmann M (2008) SIRT1 regulates circadian clock gene expression through PER2 deacetylation. Cell 134:317–328. https://doi.org/10.1016/j.cell.2008.06.050

Balsalobre A, Brown SA, Marcacci L (2000) Resetting of circadian time in peripheral tissues by glucocorticoid signaling. Science 289:2344–2347. https://doi.org/10.1126/science.289.5488.2344

Barboza PS, Farley SD, Robbins CT (1997) Whole-body urea cycling and protein turnover during hyperphagia and dormancy in growing bears (*ursus americanus* and *u.arctos*). Can J Zool 75:2129–2136. https://doi.org/10.1139/z97-848

Barger JL, Brand MD, Barnes BM, Boyer BB (2003) Tissue-specific depression of mitochondrial proton leak and substrate oxidation in hibernating arctic ground squirrels. Am J Physiol. https://doi.org/10.1152/ajpregu.00579.2002

Bass J, Takahashi JS (2010) Circadian integration of metabolism and energetics. Science 330:1349–1354. https://doi.org/10.1126/science.1195027

Bates D, Mächler M, Bolker B, Walker S (2015) Fitting linear mixed-effects models using lme4. J Stat Softw 67(1):1–48. https://doi.org/10.18637/jss.v067.i01

Battersby BJ, Moyes CD (1998) Influence of acclimation temperature on mitochondrial DNA, RNA, and enzymes in skeletal muscle. Am J Physiol. https://doi.org/10.1152/ajpregu.1998.275.3.r905

Bellet MM, Orozco-Solis R, Sahar S (2011) The time of metabolism: NAD+, SIRT1, and the circadian clock. Cold Spring Harbor Symp Quant Biol 76:31–38. https://doi.org/10.1101/sqb.2011.76.010520

Buhr ED, Yoo S-H, Takahashi JS (2010) Temperature as a universal resetting cue for mammalian circadian oscillators. Science 330:379–385

Castro-Mondragon JA, Riudavets-Puig R, Rauluseviciute I, Lemma RB, Turchi L, Blanc-Mathieu R, Lucas J, Boddie P, Khan A, Manosalva Pérez N, Fornes O, Leung TY, Aguirre A, Hammal F, Schmelter D, Baranasic D, Ballester B, Sandelin A, Lenhard B, Vandepoele K, Mathelier A (2022) JASPAR 2022: the 9th release of the open-access database of transcription factor binding profiles. Nucleic Acids Res 50(D1):D165–D173. https://doi.org/10.1093/nar/gkab1113

De Goede P, Wefers J, Brombacher EC (2018) Circadian rhythms in mitochondrial respiration. J Mol Endocrinol 60:R115–R130. https://doi.org/10.1530/jme-17-0196

Dobin A, Davis CA, Schlesinger F et al (2012) Star: Ultrafast universal RNA-seq aligner. Bioinformatics 29:15–21. https://doi.org/10.1093/bioinformatics/bts635

Dunlap JC (1999) Molecular bases for circadian clocks. Cell 96:271–290. https://doi.org/10.1016/s0092-8674(00)80566-8

Farley SD, Robbins CT (1995) Lactation, hibernation, and mass dynamics of American Black Bears and grizzly bears. Can J Zool 73:2216–2222. https://doi.org/10.1139/z95-262

Gearing LJ, Cumming HE, Chapman R (2019) CiiiDER: A tool for predicting and analysing transcription factor binding sites. PLoS ONE 14:e0215495. https://doi.org/10.1371/journal.pone.0215495

Gehring JL, Rigano KS, Evans Hutzenbiler BD (2016) A protocol for the isolation and cultivation of brown bear (Ursus arctos) adipocytes. Cytotechnology 68:2177–2191. https://doi.org/10.1007/s10616-015-9937-y

Guderley H, St-Pierre J (2002) Going with the flow or life in the fast lane: contrasting mitochondrial responses to thermal change. J Experim Biol 205:2237–2249. https://doi.org/10.1242/jeb.205.15.2237

Hapner Hogan HR, Hutzenbiler BDE, Robbins CT, Jansen HT (2022) Changing lanes: seasonal differences in cellular metabolism of adipocytes in grizzly bears (Ursus arctos horribilis). J Comp Physiol B 192:397–410. https://doi.org/10.1007/s00360-021-01428-z

Hellgren EC (1998) Physiology of hibernation in bears. Ursus 10:467–477

Hodge BA, Wen Y, Riley LA (2015) The endogenous molecular clock orchestrates the temporal separation of substrate metabolism in skeletal muscle. Skeletal Muscle. https://doi.org/10.1186/s13395-015-0039-5

Hughes ME, Hogenesch JB, Kornacker K (2010) JTK_CYCLE: an efficient nonparametric algorithm for detecting rhythmic components in genome-scale data sets. J Biol Rhythms 25:372–380. https://doi.org/10.1177/0748730410379711

Izumo M, Johnson CH, Yamazaki S (2003) Circadian gene expression in mammalian fibroblasts revealed by real-time luminescence reporting: Temperature compensation and damping. Proc Natl Acad Sci 100:16089–16094. https://doi.org/10.1073/pnas.2536313100

Jansen HT, Leise T, Stenhouse G (2016) The bear circadian clock doesn't 'sleep' during winter dormancy. Front Zool. https://doi.org/10.1186/s12983-016-0173-x

Jansen HT, Trojahn S, Saxton MW (2019) Hibernation induces widespread transcriptional remodeling in metabolic tissues of the grizzly bear. Commun Biol. https://doi.org/10.1038/s42003-019-0574-4

Jonckheere AI, Smeitink JAM, Rodenburg RJT (2012) Mitochondrial ATP synthase: architecture, function and pathology. J Inherited Metabolic Dis 35:211–225. https://doi.org/10.1007/s10545-011-9382-9

Jordan SD, Lamia KA (2013) AMPK at the crossroads of circadian clocks and metabolism. Mol Cell Endocrinol 366:163–169. https://doi.org/10.1016/j.mce.2012.06.017

Keay JA, Robbins CT, Farley SD (2018) Characteristics of a naturally regulated grizzly bear population. J Wildlife Manage 82:789–801. https://doi.org/10.1002/jwmg.21425

Korkuc P, Schippers JHM, Walther D (2013) Characterization and identification of cis-regulatory elements in Arabidopsis based on single-nucleotide polymorphism information. Plant Physiol 164:181–200. https://doi.org/10.1104/pp.113.229716

Körtner G, Geiser F (2000) The temporal organization of daily torpor and hibernation: circadian and circannual rhythms. Chronobiol Int 17:103–128. https://doi.org/10.1081/cbi-100101036

Krueger, F. (2014) Trim Galore!:A wrapper tool around Cutadapt and Fastqc toconsistently apply quality and adapter trimming to Fastqfiles

Kumar L, Futschik ME (2007) Mfuzz: A software package for soft clustering of microarray data. Bioinformation 2:5–7. https://doi.org/10.6026/97320630002005

Langfelder P, Horvath S (2008) WGCNA: an R package for weighted correlation network analysis. BMC Bioinform. https://doi.org/10.1186/1471-2105-9-559

Langfelder P, Horvath S (2012) Fast R functions for robust correlations and hierarchical clustering. J Stat Softw 46(11):1–17

Langner R, Rensing L (1972) Notizen: circadian rhythm of oxygen consumption in rat liver suspension culture: changes of pattern. Zeitschrift Für Naturforschung B 27:1117–1118. https://doi.org/10.1515/znb-1972-0945

Liao Y, Smyth GK, Shi W (2013) Featurecounts: An efficient general purpose program for assigning sequence reads to genomic features. Bioinformatics 30:923–930. https://doi.org/10.1093/bioinformatics/btt656

Liu C, Li S, Liu T (2007) Transcriptional coactivator PGC-1α integrates the mammalian clock and energy metabolism. Nature 447:477–481. https://doi.org/10.1038/nature05767

Mookerjee SA, Nicholls DG, Brand MD (2016) Determining maximum glycolytic capacity using extracellular flux measurements. PLoS ONE 11:e0152016. https://doi.org/10.1371/journal.pone.0152016

Mookerjee SA, Gerencser AA, Nicholls DG, Brand MD (2017) Quantifying intracellular rates of glycolytic and oxidative ATP production and consumption using extracellular flux measurements. J Biol Chem 292:7189–7207. https://doi.org/10.1074/jbc.m116.774471

Nelson R, Wahner H, Jones J et al (1973) Metabolism of bears before, during, and after Winter sleep. Am J Physiol Legacy Content 224:491–496. https://doi.org/10.1152/ajplegacy.1973.224.2.491

Ness-Cohn E, Iwanaszko M, Kath WL (2020) TimeTrial: an interactive application for optimizing the design and analysis of transcriptomic time-series data in circadian biology research. J Biol Rhythms 35:439–451. https://doi.org/10.1177/0748730420934672

Ptitsyn AA, Gimble JM (2011) True or false: All genes are rhythmic. Ann Med 43:1–12. https://doi.org/10.3109/07853890.2010.538078

Ramsey KM, Yoshino J, Brace CS (2009) Circadian clock feedback cycle through NAMPT-Mediated NAD + biosynthesis. Science 324:651–654. https://doi.org/10.1126/science.1171641

Ray S, Valekunja UK, Stangherlin A et al (2020) Circadian rhythms in the absence of the clock gene *bmal1*. Science 367:800–806. https://doi.org/10.1126/science.aaw7365

Revel FG, Herwig A, Garidou ML, Dardente H, Menet JS, Masson-Pévet M, Simonneaux V, Saboureau M, Pévet P (2007) The circadian clock stops ticking during deep hibernation in the European hamster. Proc Natl Acad Sci USA 104:13816–13820

Rigano KS, Gehring JL, Evans Hutzenbiler BD (2017) Life in the fat lane: seasonal regulation of insulin sensitivity, food intake, and adipose biology in brown bears. J Comp Physiol B 187:649–676. https://doi.org/10.1007/s00360-016-1050-9

Robbins CT, Lopez-Alfaro C, Rode KD et al (2012) Hibernation and seasonal fasting in bears: The energetic costs and consequences for polar bears. J Mammal 93:1493–1503. https://doi.org/10.1644/11-mamm-a-406.1

Robinson MD, McCarthy DJ, Smyth GK (2009) edger: A bioconductor package for differential expression analysis of digital gene expression data. Bioinformatics 26:139–140. https://doi.org/10.1093/bioinformatics/btp616

Ruf T (1999) The Lomb-Scargle periodogram in biological rhythm research: analysis of incomplete and unequally spaced time-series. Biol Rhythm Res 30:178–201

Rutter J, Reick M, Mcknight SL (2002) Metabolism and the control of circadian rhythms. Annu Rev Biochem 71:307–331. https://doi.org/10.1146/annurev.biochem.71.090501.142857

Saxton MW, Perry BW, Evans Hutzenbiler BD (2022) Serum plays an important role in reprogramming the seasonal transcriptional profile of brown bear adipocytes. iScience 25:105084. https://doi.org/10.1016/j.isci.2022.105084

Schmitt K, Grimm A, Dallmann R (2018) Circadian control of DRP1 activity regulates mitochondrial dynamics and bioenergetics. Cell Metab 27:657-666.e5. https://doi.org/10.1016/j.cmet.2018.01.011

Sikes RS, Gannon WL (2011) Guidelines of the American society of mammalogists for the use of wild mammals in research. J Mammal 92:235–253. https://doi.org/10.1644/10-mamm-f-355.1

Stöckel J, Welsh EA, Liberton M, Kunnvakkam R, Aurora R, Pakrasi HB (2008) Global transcriptomic analysis of Cyanothece 51142 reveals robust diurnal oscillation of central metabolic processes. Proc Natl Acad Sci 105(16):6156–6161

Storey KB (1997) Metabolic regulation in mammalian hibernation: enzyme and protein adaptations. Comp Biochem Physiol 118:1115–1124

The R project for statistical computing. In: R. https://www.r-project.org/. Accessed 16 Mar 2023.

Thiel A, Giroud S, Hertel AG et al (2022) Seasonality in biological rhythms in Scandinavian brown bears. Front Physiol 13:785706. https://doi.org/10.3389/fphys.2022.785706

Tøien Ø, Blake J, Edgar DM et al (2011) Hibernation in black bears: independence of metabolic suppression from body temperature. Science 331(6019):906–909. https://doi.org/10.1126/science.1199435

Tzagoloff A, Macino G (1979) Mitochondrial genes and translation products. Annu Rev Biochem 48:419–439. https://doi.org/10.1146/annurev.bi.48.070179.002223

Vella CA, Nelson OL, Jansen HT (2020) Regulation of metabolism during hibernation in brown bears (Ursus arctos): Involvement of cortisol, PGC-1α and AMPK in adipose tissue and skeletal muscle. Comp Biochem Physiol Part A 240:110591. https://doi.org/10.1016/j.cbpa.2019.110591

Vitaterna MH, Takahashi JS, Turek FW (2001) Overview of circadian rhythms. Alcohol Res Health 25(2):85–93

Wang G-Z, Stephanie SL (2015) Cycling transcriptional networks optimize energy utilization on a genome scale. Cell Rep 13:1868–1880. https://doi.org/10.1016/j.celrep.2015.10.043

Wang J, Vasaikar S, Shi Z et al (2017) WebGestalt 2017: A more comprehensive, powerful, flexible and interactive gene set Enrichment Analysis Toolkit. Nucleic Acids Res. https://doi.org/10.1093/nar/gkx356

Ware JV, Nelson OL, Robbins CT (2013) Endocrine rhythms in the brown bear (Ursus arctos): Evidence supporting selection for decreased pineal gland size. Physiol Rep. https://doi.org/10.1002/phy2.48

Ware JV, Rode KD, Robbins CT et al (2020) The clock keeps ticking: Circadian rhythms of free-ranging polar bears. J Biol Rhythms 35:180–194. https://doi.org/10.1177/0748730419900877

Weinrich TW, Kam JH, Ferrara BT (2019) A day in the life of mitochondria reveals shifting workloads. Sci Rep. https://doi.org/10.1038/s41598-019-48383-y

Welinder KG, Hansen R, Overgaard MT (2016) Biochemical foundations of health and energy conservation in hibernating free-ranging subadult brown bear Ursus arctos. J Biol Chem 291:22509–22523. https://doi.org/10.1074/jbc.m116.742916

Williams CT, Barnes BM, Buck CL (2012) Daily body temperature rhythms persist under the midnight sun but are absent during hibernation in free-living arctic ground squirrels. Biol Let 8:31–34. https://doi.org/10.1098/rsbl.2011.0435

Williams CT, Radonich M, Barnes BM, Buck CL (2017) Seasonal loss and resumption of circadian rhythms in hibernating arctic ground squirrels. J Comp Physiol B 187:693–703. https://doi.org/10.1007/s00360-017-1069-6

Wu G, Anafi RC, Hughes ME (2016) MetaCycle: an integrated R package to evaluate periodicity in large scale data. Bioinformatics 32:3351–3353. https://doi.org/10.1093/bioinformatics/btw405

Zhang R, Lahens NF, Ballance HI (2014) A circadian gene expression atlas in mammals: implications for biology and medicine. Proc Natl Acad Sci 111:16219–16224. https://doi.org/10.1073/pnas.1408886111

Terms and Conditions

Springer Nature journal content, brought to you courtesy of Springer Nature Customer Service Center GmbH (“Springer Nature”).
Springer Nature supports a reasonable amount of sharing of research papers by authors, subscribers and authorised users (“Users”), for small-scale personal, non-commercial use provided that all copyright, trade and service marks and other proprietary notices are maintained. By accessing, sharing, receiving or otherwise using the Springer Nature journal content you agree to these terms of use (“Terms”). For these purposes, Springer Nature considers academic use (by researchers and students) to be non-commercial.
These Terms are supplementary and will apply in addition to any applicable website terms and conditions, a relevant site licence or a personal subscription. These Terms will prevail over any conflict or ambiguity with regards to the relevant terms, a site licence or a personal subscription (to the extent of the conflict or ambiguity only). For Creative Commons-licensed articles, the terms of the Creative Commons license used will apply.
We collect and use personal data to provide access to the Springer Nature journal content. We may also use these personal data internally within ResearchGate and Springer Nature and as agreed share it, in an anonymised way, for purposes of tracking, analysis and reporting. We will not otherwise disclose your personal data outside the ResearchGate or the Springer Nature group of companies unless we have your permission as detailed in the Privacy Policy.
While Users may use the Springer Nature journal content for small scale, personal non-commercial use, it is important to note that Users may not:

1. use such content for the purpose of providing other users with access on a regular or large scale basis or as a means to circumvent access control;
2. use such content where to do so would be considered a criminal or statutory offence in any jurisdiction, or gives rise to civil liability, or is otherwise unlawful;
3. falsely or misleadingly imply or suggest endorsement, approval , sponsorship, or association unless explicitly agreed to by Springer Nature in writing;
4. use bots or other automated methods to access the content or redirect messages
5. override any security feature or exclusionary protocol; or
6. share the content in order to create substitute for Springer Nature products or services or a systematic database of Springer Nature journal content.

In line with the restriction against commercial use, Springer Nature does not permit the creation of a product or service that creates revenue, royalties, rent or income from our content or its inclusion as part of a paid for service or for other commercial gain. Springer Nature journal content cannot be used for inter-library loans and librarians may not upload Springer Nature journal content on a large scale into their, or any other, institutional repository.
These terms of use are reviewed regularly and may be amended at any time. Springer Nature is not obligated to publish any information or content on this website and may remove it or features or functionality at our sole discretion, at any time with or without notice. Springer Nature may revoke this licence to you at any time and remove access to any copies of the Springer Nature journal content which have been saved.
To the fullest extent permitted by law, Springer Nature makes no warranties, representations or guarantees to Users, either express or implied with respect to the Springer nature journal content and all parties disclaim and waive any implied warranties or warranties imposed by law, including merchantability or fitness for any particular purpose.
Please note that these rights do not automatically extend to content, data or other material published by Springer Nature that may be licensed from third parties.
If you would like to use or distribute our Springer Nature journal content to a wider audience or on a regular basis or in any other manner not expressly permitted by these Terms, please contact Springer Nature at

onlineservice@springernature.com